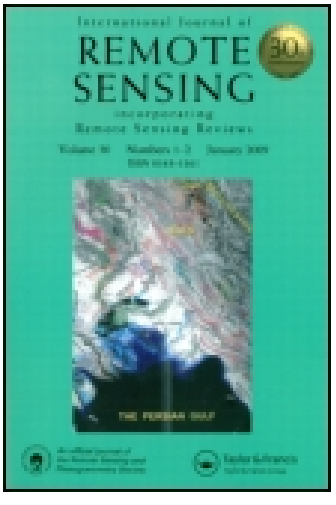

International Journal of Remote Sensing

Publication details, including instructions for authors and subscription information:
http://www.tandfonline.com/loi/tres20

Estimation of atmospheric particulate matter based on MODIS haze optimized transformation

Qiao Wang [a] , Yong Zha [b] , Jay Gao [c] & Dan Shen [b]

[a] Satellite Environment Centre , Ministry of Environmental Protection , Beijing , 100094 , China

[b] Key Laboratory of Virtual Geographic Environment of Ministry of Education, College of Geographic Science , Nanjing Normal University , Nanjing , 210097 , China

[c] School of Geography, Geology and Environmental Science , University of Auckland , Auckland , 1008 , New Zealand

Published online: 05 Nov 2012.

To cite this article: Qiao Wang , Yong Zha , Jay Gao & Dan Shen (2013) Estimation of atmospheric particulate matter based on MODIS haze optimized transformation, International Journal of Remote Sensing, 34:5, 1855-1865, DOI: 10.1080/01431161.2012.730155

To link to this article: http://dx.doi.org/10.1080/01431161.2012.730155

International Journal of Remote Sensing
Vol. 34, No. 5, 10 March 2013, 1855–1865

Taylor & Francis
Taylor & Francis Group

Estimation of atmospheric particulate matter based on MODIS haze optimized transformation

Qiao Wang[a], Yong Zha[b]*, Jay Gao[c], and Dan Shen[b]

[a]*Satellite Environment Centre, Ministry of Environmental Protection, Beijing 100094, China;* [b]*Key Laboratory of Virtual Geographic Environment of Ministry of Education, College of Geographic Science, Nanjing Normal University, Nanjing 210097, China;* [c]*School of Geography, Geology and Environmental Science, University of Auckland, Auckland 1008, New Zealand*

(*Received 5 October 2011; accepted 28 June 2012*)

This research is an attempt to simulate the relationship between haze optimized transformation (HOT) and aerosol optical thickness (AOT), and explore the influence of typical ground covers on this relationship using the 6S atmospheric radiative transfer model for the Chinese city of Nanjing. The HOT data were derived from moderate resolution imaging spectroradiometer (MODIS) satellite images recorded in the winter and spring seasons of December 2007–May 2009. They were analysed in conjunction with ground observed atmospheric particulate matter (PM) data so as to establish their quantitative relationship. Such a relationship may open a new avenue for remotely estimating atmospheric PM based on HOT. The results obtained indicate that HOT is related positively to AOT. This relationship is most accurately depicted by a second-order polynomial equation. Although built-up areas, waterbodies, and vegetation have differing HOT values, all of them bear a close and consistent correlation with AOT. HOT of built-up areas, waterbodies, and vegetative surfaces derived from MODIS images is also positively correlated with PM_{10} (PM with diameter <10 μm), which was measured near the surface. The second-order polynomial equation has a coefficient of determination (R^2) value of 0.375 (built-up), 0.344 (water), and 0.362 (vegetation) and a root mean squared error (RMSE) of 0.0258, 0.0264, and 0.0261, respectively. The closeness in R^2 value and RMSE for different ground covers suggests that correlation is marginally affected by the ground cover. It is thus concluded that HOT can be used as a reliable alternative for estimating PM_{10} from MODIS data.

1. Introduction

Since the beginning of the twentieth century, an increasing quantity of pollutants has been produced daily around the world as a consequence of rapid industrialization and urbanization. The release of such pollutants into the atmosphere with little treatment has severely degraded air quality and posed grave threats to human health. Serious atmospheric pollution has caused many environmental problems (e.g. acid rain), and is blamed for surging respiratory cases around the world (Cyrys et al. 2005). Atmospheric pollution is an especially serious problem in developing countries. As the largest developing country in the world, China also faces the same serious problem of air pollution that has been exacerbated by the rapid pace of economic development and urbanization.

*Corresponding author. Email: yzha@njnu.edu.cn

ISSN 0143-1161 print/ISSN 1366-5901 online

http://dx.doi.org/10.1080/01431161.2012.730155
http://www.tandfonline.com

All pollutants in the atmosphere fall into two broad categories: gaseous and particulate pollutants. The latter are the major pollutants in most Chinese cities. Therefore, it is important to control their release into the atmosphere in order to ameliorate poor air quality. At present, monitoring of particulate pollutants in the atmosphere is usually accomplished via two means, namely, ground measurement and satellite surveillance. The former relies on a network of ground observation stations at which air pollutant concentration and its temporal variation are recorded manually or automatically. Most of the ground observation stations in China are distributed in urban areas. These stations are able to yield accurate measurements in a timely fashion. Nevertheless, the observed data are unable to capture the spatial variation of pollutants over a broad scale owing to the limited number of observation stations. By comparison, satellite monitoring is advantageous for its capacity for real-time and dynamic surveillance over extensive areas. Such strengths make satellite data a vital source in studying the spatiotemporal variations of atmospheric pollutants. In fact, space-borne remote sensing has become one of the most important means of monitoring air pollution. In particular, satellite data of improved temporal resolution and multi-functional satellites such as moderate resolution imaging spectroradiometer (MODIS) data have played a critical role in assessing air pollution. Over recent years, MODIS data have found wide applications in estimating particulate pollutants in the atmosphere at a scale ranging from regional to global (Chu et al. 2003; Engel-Cox et al. 2004; Gupta et al. 2006, 2007). The common approach of estimation is to first establish a statistical relationship between satellite-retrieved aerosol optical thickness (AOT) and ground-measured concentration levels of particulate matter (PM). This relationship is then applied to yield estimates of atmospheric pollutants for a given AOT. A positive correlation between the two variables has been reported by a few scientists (Wang and Christopher 2003; Hutchison, Smith, and Faruqui 2005; Vidot, Santer, and Ramon 2007; Di Nicolantonio, Cacciari, and Tomasi 2009). However, AOT is by no means synonymous with the concentration of ground-measured PM. Actually, each has its own unique physical meaning. AOT signifies the vertically integrated aerosol extinction that optically quantifies the aerosol load in the whole atmospheric column. It is related to the total particular matter in the vertical direction. The mass concentration of ground-measured particular matter represents aerosols near the Earth's surface. It is strongly influenced by atmospheric conditions. Therefore, the correlation between these two variables is also strongly subject to seasonality and meteorological conditions. It is thus recommended that separate relationships between PM and AOT be established by seasons or under different meteorological conditions (Barnaba et al. 2010; Tian and Chen 2010b; Zha et al. 2010), or through the incorporation of ground-level temperature and relative humidity (Li et al. 2005; Tian and Chen 2010a; Wang et al. 2010) so as to improve model accuracy. Despite the feasibility of estimating atmospheric PM from satellite imagery based on its relationship with AOT, the inversion process is rather complex. Besides, some data such as the MODIS AOT products are available only at 10 km resolution. Such a coarse spatial resolution sometimes cannot meet the needs in estimating atmospheric particulates.

As a manifestation of severe pollution, haze is formed when the quantity of particles suspended in the atmosphere exceeds a certain level with a corresponding decrease in visibility. Using surface reflectance data collected from different covers in Canada with the assistance of an atmospheric radiative transfer model known as MODTRAN (Moderate Resolution Atmospheric Transmission), Zhang, Guindon, and Cihlar (2002) simulated the variation in apparent reflectance under different ground covers in the 2D spectral domain of Landsat Thematic Mapper band 1 (TM1) (blue band, horizontal axis) and band 3 (TM3) (red band, vertical axis) under ever increasing AOT. Their results indicate that surface

reflectances of different ground covers under clear-sky conditions are highly correlated with each other (correlation coefficient = 0.993) in this spectral domain. This correlation line is termed the 'clear line'. With the increase in AOT, apparent reflectance values in both TM1 and TM3 rise. However, apparent reflectance in the blue band rises at a faster pace than its counterpart in the red band. Thus, apparent reflectance gradually deviates from the 'clear line' towards the upper right of the graph at a larger AOT. In fact, the larger the AOT, the greater the deviation. Therefore, the distance from apparent reflectance to the 'clear line' is indicative of AOT. This distance, named haze optimized transformation (HOT), can be defined as:

$$\mathrm{HOT} = B_1 \sin\theta - B_3 \cos\theta, \tag{1}$$

where B_1 and B_3 stand for the apparent reflectance values in TM1 and TM3, respectively, and θ refers to the inverse tangent of the slope of the 'clear line'.

HOT was intended initially to detect and eliminate haze or thin clouds from Landsat TM/ETM+ (Enhanced Thematic Mapper Plus) images (Zhang, Guindon, and Cihlar 2002; Zhang and Guindon 2003). Lately, improved HOT has been applied as a means of atmospheric correction, with satisfactory results (He et al. 2010). In this study, the ability of HOT to estimate particular pollutants in the atmosphere from MODIS satellite data was tested and evaluated for the Chinese city of Nanjing. With the assistance of the 6S atmospheric radiative transfer model, we analysed the relationship between HOT and AOT, and explored the influence of typical ground covers on this relationship. Furthermore, we also analysed the relationship between HOT derived from MODIS satellite data and the concentration of atmospheric particulate pollutants measured near the Earth's surface so as to establish a remote-sensing model for estimating atmospheric pollutants via HOT. Such a model has the potential to become a new avenue for monitoring atmospheric pollutants from space.

2. Study area

The study site, Nanjing City, is located in the prosperous Yangtze River delta. Its favourable geographical location in the lowest reach of the Yangtze River has made it a critical economic centre and a major industrial metropolis, as well as an important transportation hub. The selected study site includes its urban areas and suburban districts while the two counties under its administration are excluded (Figure 1). This selection is based on the consideration of its diverse ground covers, as well as a wide range of geomorphic units, such as low-lying hills, mountains, broad valleys, lacustrine plains, and river terraces. More importantly, the city has been plagued by a chronic air pollution problem that has worsened over the last few decades.

Atmospheric pollutants in Nanjing can be traced back to three leading sources: industrial plants, construction sites and vehicles, and agriculture. The industrial area that has caused profound air pollution in Nanjing is confined to the north of the city. It has a high concentration of heavy industries that produce massive gaseous wastes annually. Moreover, its location in the upwind of predominant winds during winters means the gaseous wastes released by these industries severely degrade the air quality of the city. Coming to the second source of atmospheric pollutants, with the ever quickening pace of urbanization, numerous construction sites distributed throughout the city and the ever expanding fleet of private motor vehicles have also contributed a significant quantity of air pollutants. Lastly, a considerable amount of particulate pollutants in the atmosphere originates from the burning of crop residues and stalks in the adjoining rural areas. However, this source of pollution is

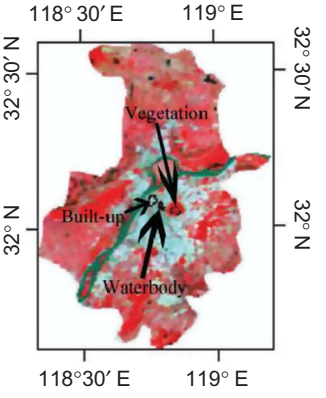

Figure 1. Location of the study site. The figure shows a false colour composite image of MODIS band 2 (red), MODIS band 1 (green), and MODIS band 4 (blue). Red is vegetation, grey is built-up areas, green is river, and black is waterbodies. The polygons in the middle show areas classified as built-up areas, waterbodies, and vegetation.

restricted to only May and October of each year following the harvest season. Air pollution by PM has become the chief characteristic of pollution in Nanjing just like in most other cities in China, with the level of pollution more severe in winter and spring than in summer and autumn (Huang et al. 2002). The PM with diameter <10 μm (PM_{10}) makes up 88.8% of the total suspended particles, and hence is a major contributor to the AOT at the study area (Wang et al. 2003).

3. Method

3.1. MODIS data used

The MODIS sensor is a major instrument aboard the Earth Observation System Terra and Aqua satellites. Terra orbits around the Earth from north to south across the equator in the morning, while Aqua passes south to north over the equator in the afternoon. With a swath width of 2330 km, MODIS imagery provides a global coverage every 1–2 days. Its broad spectrum extends from 0.405 to 14.385 μm in 36 wavebands. All MODIS bands have a spatial resolution of 250, 500, or 1000 m. MODIS data are characterized by their huge quantity, comprehensive coverage, fast updating, and longitudinal comparability. As such, they have become a reliable source for monitoring natural disasters and studying global climate change and atmospheric pollution.

Apart from MODIS data themselves, many products have also been derived from them, all of which are freely available to the public. The MODIS products used in this research include MOD02HKM and MOD03 downloaded from http://ladsweb.nascom.nasa.gov/, and MCD43A4 downloaded from https://lpdaac.usgs.gov/. MOD02HKM contains calibrated but not geometrically corrected radiance and reflectance at a spatial resolution of 500 m. MOD03 is the 1 km geolocation product that encompasses azimuth and zenith angles of the Sun and the satellite. MCD43A4 provides 500 m reflectance data that have been adjusted using a bidirectional reflectance distribution function to model the values as if they were taken from the nadir view. The MCD43A4 product contains 16 day gridded data with a sinusoidal projection. Both Terra and Aqua data are used in the generation of this product, providing the highest probability for quality input data.

All MOD02HKM, MOD03, and MCD43A4 data recorded in the winter and spring of December 2007–May 2009 were collected. Of these data, cloud-free MOD02HKM

and MOD03 scenes total 80. They were processed in several steps, including geometric correction, spatial resolution unification via resampling, and subsetting, to derive the required results. Specifically, MOD02HKM and MOD03 were geometrically projected to the Universal Transverse Mercator (UTM) system (zone 50N; datum: WGS-84). The MOD03 product was resampled to 500 m to be compatible with that of MOD02HKM. The MCD43A4 product was converted to UTM, the same for MOD02HKM and MOD03. All three sets of images (i.e. geometrically corrected MOD02HKM and MOD03, and MCD43A4) were subset via intersection with the same boundary of an identical projection to define the study site.

3.2. PM_{10} determination

The PM_{10} data needed in this study were converted from the air pollution index (API) downloaded from the (Chinese) Ministry of Environmental Protection website (http://english.mep.gov.cn/). API is an index easily comprehensible to the public. It corresponds to the concentration levels of PM_{10}, sulphur dioxide (SO_2), and other pollutants. The API for a given day was calculated individually from all major pollutants and the maximum API among all pollutants was considered the ultimate figure for this day. Therefore, it is possible to retrieve PM_{10} from API if the pollutants are dominated by PM_{10} on this day. Over the 80 days when cloud-free MODIS MOD02HKM and MOD03 data were available, the chief pollutants were indeed dominated by PM_{10}. Therefore, PM_{10} was derived from API based on the following conversion relationship:

$$\mathrm{API} = (\mathrm{PM}_{10-50})(100-50)/(150-50)+50 \text{ if } 50 < \mathrm{PM}_{10} < 150\ \mu\mathrm{g\,m}^{-3}, \quad (2)$$

$$\mathrm{API} = (\mathrm{PM}_{10-150})(200-100)/(350-150)+100 \text{ if } 150 < \mathrm{PM}_{10} < 350\ \mu\mathrm{g\,m}^{-3}, \quad (3)$$

$$\mathrm{API} = (\mathrm{PM}_{10-350})(300-100)/(420-350)+200 \text{ if } 350 < \mathrm{PM}_{10} < 420\ \mu\mathrm{g\,m}^{-3}. \quad (4)$$

3.3. HOT derivation

If HOT is applied to monitoring atmospheric pollution, it is advisable to use satellite data that have a temporal resolution finer than 16 days for TM imagery, such as MODIS data. Since the resolution of MODIS satellite data is 250 m at best, much coarser than the 30 m for TM, it is occasionally impossible to derive the 'clear line' reliably using a small cloud-free subset image as Zhang, Guindon, and Cihlar (2002) did, especially when the study site has a limited spatial dimension. It was circumvented by taking advantage of the relationship between the surface reflectance of the red and blue wavebands contained in MODIS MCD43A4. The mean surface reflectance in the red and blue wavebands was calculated for the winter and spring seasons, respectively. Under clear-sky conditions, there also exists a linear relationship between the surface reflectance of ground objects on MODIS blue and red bands (Figure 2), similar to that with the TM data reported by Zhang, Guindon, and Cihlar (2002). Moreover, with the increase in AOT, apparent reflectance gradually deviates from the 'clear line', or HOT has an ever increasing value. Therefore, it is possible to estimate the variation of aerosols in the atmosphere via MODIS HOT.

After the existence of this 'clear line' is confirmed, the next step is to determine θ, which is essential in computing HOT from Equation (1). θ is the inverse tangent of the slope of the linear regression relationship between surface reflectance in the red and blue wavebands. The apparent reflectance in the red and blue wavebands was determined with

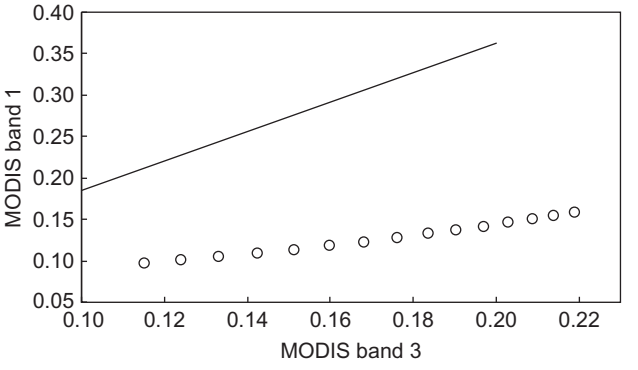

Figure 2. Variation in the apparent reflectance of MODIS bands 1 (red) and 3 (blue) under different AOTs (from left to right at an interval of 0.1 over the range of 0.1–1.5) (the solid line is the clear line).

the assistance of the 6S atmospheric radiative transfer model after a number of parameters (e.g. geometry of the Sun and the satellite, atmospheric model, aerosol type, AOT, and surface reflectance) were plugged into the model. As an example, in the winter season, the solar and satellite zeniths were taken as 45° and 30°, respectively. Both have a difference of 120° in azimuth angle. The atmospheric model was mid-latitude winter and the aerosol type was continental. Over the range of 0.1–1.5, AOT has an increment of 0.1. The surface reflectance in the red and blue wavebands is 0.088 and 0.045, respectively (the mean value over the study area). Thus, the simulated HOT was determined using Equation (1).

The apparent reflectance needed in deriving HOT from the MODIS data was calculated by dividing the reflectance in MOD02HKM by cos θ_z (θ_z refers to the solar zenith angle available from MOD03). MODIS HOT was hence determined based on Equation (1).

4. Results

4.1. θ values

Figure 3 is a 2D scatterplot of reflectance in the MODIS blue band (*x*-axis) and the MODIS red band (*y*-axis). It illustrates the mean surface reflectance in the winter and spring seasons. Statistical regression analysis reveals that the two sets of reflectance have a correlation coefficient of 0.96 in the winter season and 0.90 in the spring season. The two regression lines have slopes (tan θ) of 1.78 and 1.58, respectively. They correspond to angles, θ, of 60.63° and 57.61°, respectively.

4.2. Relationship between AOT and simulated HOT

Figure 4 illustrates the relationship between simulated HOT and AOT. Apparently, HOT rises with the increment in AOT. This positive relationship was fitted with five types of curves, including linear, logarithmic, second-order polynomial, power, and exponential. Of these five equations, the second-order polynomial is the most accurate, achieving an R^2 value of 0.9999.

In order to explore the influence of ground covers on the above relationship, more simulations were carried out with three typical ground covers, namely, built-up areas, waterbodies, and vegetation (Figure 1). They have corresponding reflectances of

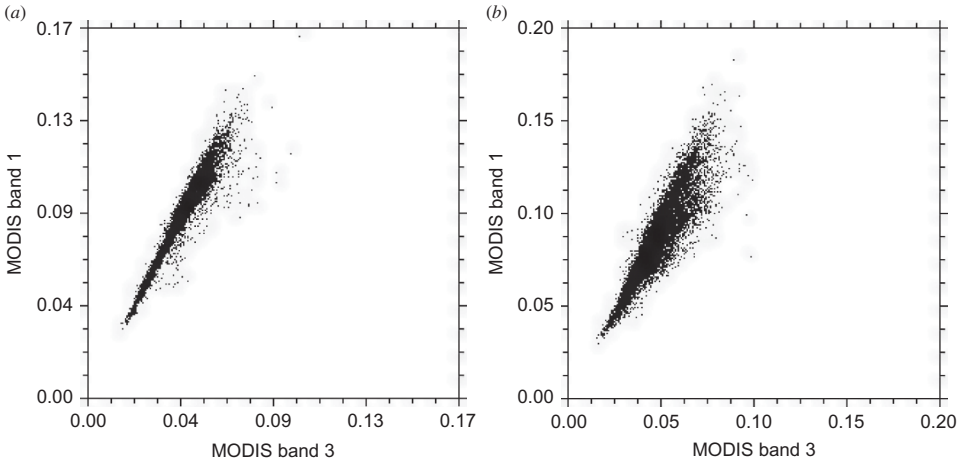

Figure 3. Scatterplots of surface reflectance in MODIS1 (red) and MODIS3 (blue) bands in two seasons: (*a*) winter and (*b*) spring.

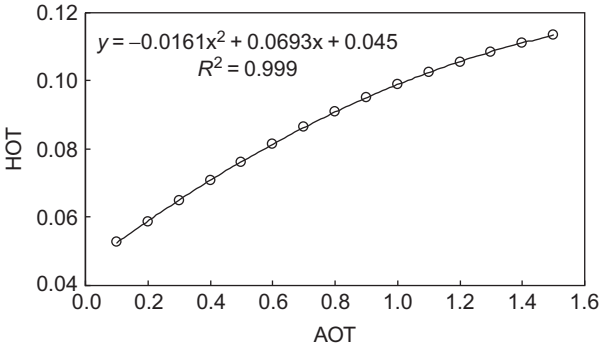

Figure 4. Relationship between simulated HOT and AOT.

0.085, 0.067, and 0.055 in the red waveband and 0.042, 0.042, and 0.028 in the blue waveband, respectively. All other parameters in the model remained unchanged in the simulations.

As illustrated in Figure 5, there is a slight difference in HOT among the three typical ground covers at a given AOT. Waterbodies have the largest HOT, followed by vegetation. Built-up areas have the lowest HOT. With the increment in AOT, the disparity in HOT among the three ground covers gradually diminishes. Such a relationship suggests that HOT is somehow sensitive to AOT for a given ground cover. Therefore, a similar polynomial relationship between AOT and HOT was established separately for each of the three ground covers. Surprisingly, all three equations achieved the same level of fitness ($R^2 = 1$). Such a close relationship indicates that estimation of AOT from simulated HOT is not subject to the influence of ground covers. A similar level of accuracy can be achieved regardless of the ground cover.

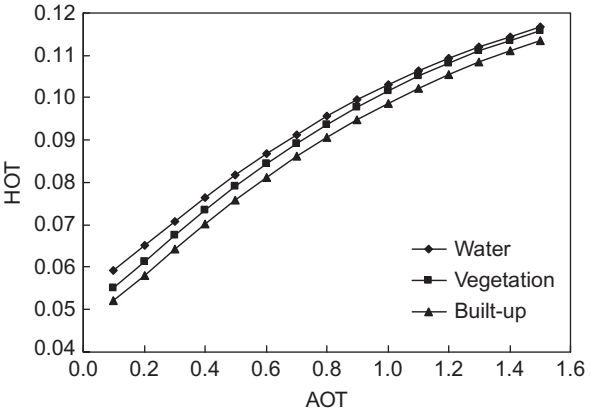

Figure 5. Variation of HOT with AOT for three typical types of ground cover in the study area.

4.3. Estimation of PM_{10} from MODIS HOT

After HOT images were produced from the processed MODIS red and blue wavebands showing apparent reflectance, and the θ angle in winter and spring, they were used to derive the pixel value of built-up areas (27 pixels), waterbodies (11 pixels), and vegetation (28 pixels). Statistical analysis revealed that the HOT values of built-up areas, vegetation, waterbodies, and all covers (e.g. a mixture of all of them) are all positively correlated with PM_{10} at coefficients of 0.613, 0.586, 0.599, and 0.601, respectively. Such correlation was tested to be statistically significant at the 0.01 level. The close similarity in the first three coefficients suggests once again that ground covers exert little influence on the accuracy of estimating PM_{10} from HOT.

In order to estimate PM_{10} from HOT, it was regressed against the independent variable of HOT for the three kinds of ground cover (built-up, water, and vegetation) as well as their mixture separately. The scatterplot between PM_{10} and HOT suggests that the second-order polynomial is the most appropriate (Figure 6). Comparison of this model with other linear, logarithmic, power, and exponential models confirms that it is also the most accurate. Such regression models have R^2 values of 0.3753, 0.3438, 0.3621, and 0.3618, respectively, for the four types of ground cover. Their corresponding root mean squared errors (RMSEs) are 0.0258, 0.0264, 0.0261, and 0.0261, respectively. These results indicate that ground covers exert little influence on the accuracy of estimating PM_{10} from HOT. Moreover, they are highly consistent with those results derived using the 6S atmospheric radiative transfer model presented in Section 4.2.

5. Discussion

MODIS HOT is only loosely correlated with PM_{10}. Their second-order polynomial equation has an R^2 value of about 0.36, much lower than the R^2 of 0.99 for that between simulated HOT and AOT. There are three possible explanations for such a large disparity. First, HOT manifests mostly the variations in AOT. Thus, simulated HOT bears a close relationship with AOT ($R^2 = 0.99$). In estimating PM_{10}, the differential meanings of AOT and PM_{10} must also degrade the positive correlation between MODIS HOT and PM_{10}. This is reminiscent of the sometimes loose correlation between AOT and PM_{10}. Secondly, the same θ angle was applied for the entire season in deriving MODIS HOT. Thirdly, there is a slight spatiotemporal mismatch between PM_{10} and MODIS HOT. The former is measured

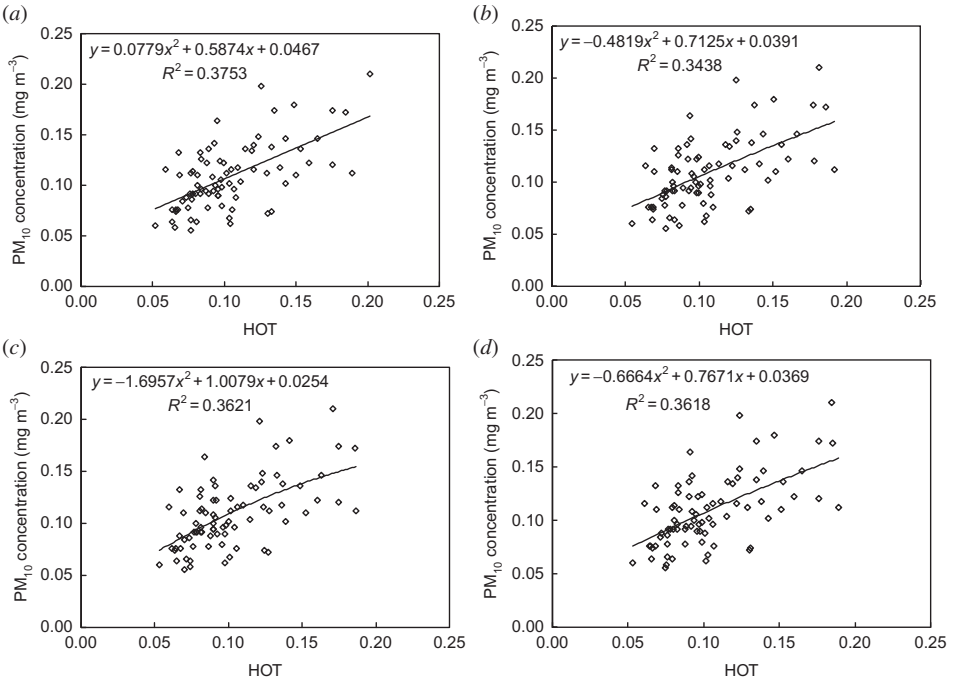

Figure 6. Second-order polynomial regression models for PM_{10} from HOT for various types of ground covers: (*a*) built-up areas; (*b*) waterbodies; (*c*) vegetation; and (*d*) mixed covers.

at a specific location for the entire day, while MODIS HOT refers to the specific moment of satellite overpass. It is obtained over a spatial extent instead of at a point.

Although HOT is related to AOT and indicative of AOT variation, the HOT approach proposed in this article differs from the MODIS V5 and Deep Blue AOT algorithms. The MODIS V5 AOT algorithm makes use of the 2.1 μm waveband in deriving surface reflectance in the red and blue bands. AOT is determined from the constructed look-up table. This method is applicable to sites with dark surface targets only. The Deep Blue AOT algorithm is able to derive AOT over bright surfaces, such as glint (over ocean), deserts (over land), ice, snow, and clouds. By comparison, HOT is calculated from apparent reflectance in the red and blue bands using Equation (1). On the other hand, apparent reflectance is subject to the influence of different factors, such as surface reflectivity and aerosol composition. Therefore, it needs to be acknowledged that the relationship between HOT and AOT will be dependent on the ability of the 6S radiative transfer model to capture the spectral dependence of surface reflectivity (which is difficult) and assumptions about the aerosol composition.

6. Conclusions

In this study, the relationship between HOT and AOT was simulated using the 6S atmospheric radiative transfer model. Based on this relationship, the PM_{10} concentration over the Chinese city of Nanjing was estimated from MODIS-derived HOT. The results demonstrate that simulated HOT is positively correlated with AOT. This relationship is best described by a second-order polynomial equation in the form of $HOT = -0.0161(AOT)^2 + 0.0693(AOT) + 0.0457$ ($R^2 = 0.9999$). This relationship varies slightly with ground covers. Nevertheless, the disparity in HOT among different ground

covers diminishes at a higher AOT. By comparison, the accuracy of estimating AOT from HOT does not vary with ground covers noticeably. HOT of built-up areas, waterbodies, and vegetation derived from the MODIS data is also positively correlated with ground-measured PM_{10} that has been converted from API. This relationship is most accurately fitted via a second-order polynomial equation. The accuracy of simulation is similarly high at an R^2 of around 0.36 for all three ground covers. The RMSE of all four models (three individual covers and one mixed cover) also has a small range of variation. Such outcomes are highly consistent with those obtained using the 6S atmospheric radiative transfer model. It is thus concluded that HOT can be used as a reliable alternative for estimating PM_{10} when it is the predominant pollutant in the atmosphere. Such a model has the potential to become a new method of monitoring atmospheric pollutants by means of remote sensing.

Acknowledgements

We thank the two anonymous reviewers for their helpful comments. The data used in this study were acquired as part of the NASA's Earth Science Enterprise. The algorithms were developed by the MODIS Science Teams. The data were processed by the MODIS Adaptive Processing System (MODAPS) and Goddard Distributed Active Archive Center (DAAC), and are archived and distributed by the Goddard DAAC. This research was funded by the National Natural Science Foundation of China (No. 41271382), the National Science and Technology Support Plan of China (No. 2008BAC34B07), the Key Fundamental Research Projects of Natural Science in Universities affiliated with the Jiangsu Province (No. 08KJA170001), the '211' Key Discipline Construction Project, the Key Short-term Projects of Inviting Overseas Experts to the Nanjing Normal University, and a project funded by the Priority Academic Programme Development of Jiangsu Higher Education Institutions, China.

References

Barnaba, F., J. P. Putaud, C. Gruening, A. Dell'acqua, and S. Dos Santos. 2010. "Annual Cycle in Co-Located *in situ*, Total-Column, and Height-Resolved Aerosol Observations in the Po Valley (Italy): Implications for Ground-Level Particulate Matter Mass Concentration Estimation from Remote Sensing." *Journal of Geophysical Research* 115: D19209. doi:10.1029/2009JD013002.

Chu, D. A., Y. J. Kaufman, G. Zibordi, J. D. Chern, J. Mao, C. C. Li, and B. N. Holben. 2003. "Global Monitoring of Air Pollution Over Land from the Earth Observing System-Terra Moderate Resolution Imaging Spectroradiometer (MODIS)." *Journal of Geophysical Research* 108: 4661. doi:10.1029/2002JD003179.

Cyrys, J., M. Hochadel, U. Gehring, G. Hoek, V. Diegmann, B. Brunekreef, and J. Heinrich. 2005. "GIS-Based Estimation of Exposure to Particulate Matter and NO_2 in an Urban Area: Stochastic Versus Dispersion Modeling." *Environmental Health Perspectives* 113: 987–92.

Di Nicolantonio, W., A. Cacciari, and C. Tomasi. 2009. "Particulate Matter at Surface: Northern Italy Monitoring Based on Satellite Remote Sensing, Meteorological Fields, and *in-situ* Samplings." *IEEE Journal of Selected Topics in Applied Earth Observations and Remote Sensing* 2: 284–92.

Engel-Cox, J. A., C. H. Holloman, B. W. Coutant, and R. M. Hoff. 2004. "Qualitative and Quantitative Evaluation of MODIS Satellite Sensor Data for Regional and Urban Scale Air Quality." *Atmospheric Environment* 38: 2495–509.

Gupta, P., S. A. Christopher, M. A. Box, and G. P. Box. 2007. "Multi Year Satellite Remote Sensing of Particulate Matter Air Quality over Sydney, Australia." *International Journal of Remote Sensing* 28: 4483–98.

Gupta, P., S. A. Christopher, J. Wang, R. Gehrig, Y. Lee, and N. Kumar. 2006. "Satellite Remote Sensing of Particulate Matter and Air Quality Assessment over Global Cities." *Atmospheric Environment* 40: 5880–92.

He, X. Y., J. B. Hu, W. Chen, and X. Y. Li. 2010. "Haze Removal Based on Advanced Haze-Optimized Transformation (AHOT) for Multispectral Imagery." *International Journal of Remote Sensing* 31: 5331–48.

Huang, L.-M., G.-H. Wang, H. Wang, S.-X. Gao, and L.-S. Wang. 2002. "Pollution Level of the Airborne Particulate Matter (PM_{10}, $PM_{2.5}$) in Nanjing City." *China Environmental Science* 22: 334–7.

Hutchison, K. D., S. Smith, and S. J. Faruqui. 2005. "Correlating MODIS Aerosol Optical Thickness Data with Ground-Based $PM_{2.5}$ Observations across Texas for Use in a Real-Time Air Quality Prediction System." *Atmospheric Environment* 39: 7190–203.

Li, C. C., J. T. Mao, A. K. H. Lau, Z. B. Yuan, M. H. Wang, and X. Y. Liu. 2005. "Application of MODIS Satellite Products to the Air Pollution Research in Beijing." *Science in China D* 48, Suppl. II: 209–19.

Tian, J., and D. M. Chen. 2010a. "A Semi-Empirical Model for Predicting Hourly Ground-Level Fine Particulate Matter (PM(2.5)) Concentration in Southern Ontario from Satellite Remote Sensing and Ground-Based Meteorological Measurements." *Remote Sensing of Environment* 114: 221–9.

Tian, J., and D. M. Chen. 2010b. "Spectral, Spatial, and Temporal Sensitivity of Correlating MODIS Aerosol Optical Depth with Ground-Based Fine Particulate Matter (PM(2.5)) across Southern Ontario." *Canadian Journal of Remote Sensing* 36: 119–28.

Vidot, J., R. Santer, and D. Ramon. 2007. "Atmospheric Particulate Matter (PM) Estimation from SeaWiFS Imagery." *Remote Sensing of Environment* 111: 1–10.

Wang, H., G. Wang, S. Gao, and L. Wang. 2003. "Characteristics of Atmospheric Particulate Pollution in Spring in Nanjing City." *China Environmental Science* 23: 55–9.

Wang, J., and S. A. Christopher. 2003. "Intercomparison between Satellite-Derived Aerosol Optical Thickness and $PM_{2.5}$ Mass: Implications for Air Quality Studies." *Geophysical Research Letters* 30: 2095. doi:10.1029/2003GL018174.

Wang, Z. F., L. F. Chen, J. H. Tao, Y. Zhang, and L. Su. 2010. "Satellite-Based Estimation of Regional Particulate Matter (PM) in Beijing Using Vertical-and-RH Correcting Method." *Remote Sensing of Environment* 114: 50–63.

Zha, Y., J. Gao, J. J. Jiang, H. Lu, and J. Z. Huang. 2010. "Monitoring of Urban Air Pollution from MODIS Aerosol Data: Effect of Meteorological Parameters." *Tellus B* 62: 109–16.

Zhang, Y., and B. Guindon. 2003. "Quantitative Assessment of a Haze Suppression Methodology for Satellite Imagery: Effect on Land Cover Classification Performance." *IEEE Transactions on Geoscience and Remote Sensing* 41: 1082–9.

Zhang, Y., B. Guindon, and J. Cihlar. 2002. "An Image Transform to Characterize and Compensate for Spatial Variations in Thin Cloud Contamination of Landsat Images." *Remote Sensing of Environment* 82: 173–87.